Impact of a pressurized membrane: Coefficient of restitution

Baptiste Darbois Texier ⃝
Université Paris-Saclay, CNRS, FAST, 91405 Orsay, France

Loïc Tadrist ⃝*
Aix-Marseille Université, CNRS, ISM, Marseille, France

Pressurized membranes are usually used for low cost structures (e.g., inflatable beds), impact protections (e.g., airbags), or sport balls. The last two examples deal with impacts on the human body. Underinflated protective membranes are not effective whereas overinflated objects can cause injury at impact. The coefficient of restitution represents the ability of a membrane to dissipate energy during an impact. Its dependence on membrane properties and inflation pressure is investigated on a model experiment using a spherical membrane. The coefficient of restitution increases with inflation pressure but decreases with impact speed. For a spherical membrane, it is shown that kinetic energy is lost by transfer to vibration modes. A physical modeling of a spherical membrane impact is built considering a quasistatic impact with small indentation. Finally, the dependency of the coefficient of restitution with mechanical parameters, pressurization, and impact characteristics is given.

I. INTRODUCTION

Pressurized elastic shells are ubiquitous, whether as natural or artificial systems. The latter case includes airbags [1], inflated helmets [2], inflated shoes [3,4], airbag suits [5], inflatable structures [6,7], and sport balls [8]. The inflation pressure allows one to adjust the mechanical properties of these systems, as an increase in pressure increases the rigidity of the shell. The fact that the mechanical properties of these systems can be easily changed makes them suitable for the interaction with humans and in particular for protection against impacts.

The mechanical response of pressurized shells has been investigated in the limit of quasistatic deformations. A pressurized spherical shell indented locally has been shown to experience a wrinkling instability above a critical indentation [9]. This observation was rationalized by considering that the overpressure introduces an effective bending stiffness in the system that competes with the natural bending stiffness of the shell. The wrinkling pattern that develops above the instability threshold was later captured by a linear stability analysis of the problem [10].

The limit of rapid deformations has been extensively studied in the case of a pressurized membrane impacting a rigid substrate [11]. In this situation, the contact dynamics between the pressurized shell and the substrate can be characterized by a coefficient of restitution. This quantity corresponds to the ratio between the ingoing speed and the outgoing speed $\eta = |U_{\text{out}}/U_0|$. The coefficient of restitution reflects the loss of kinetic energy during the impact. η is unity for lossless impacts. However, the simplicity of the definition of the coefficient of restitution masks the multiple possible physical

origins of energy loss for a pressurized membrane. A fraction of the membrane kinetic energy may be transferred to (i) membrane vibrations [12], (ii) the ambient media vibrations (sound [13] and ground vibrations), heat converted by (iii) viscous dissipation in the membrane, (iv) friction with the ground, or (v) thermally exchanged during impact (nonadiabatic compression-expansion cycle of the internal gas). Deciphering between those physical origins of energy dissipation will shape a theory to predict the evolution of coefficient of restitution with inflation pressure, membrane mechanical parameters, and impact speed.

Specifically for spherical shells, two different physical explanations have been proposed to account for the loss of energy during the impact of a pressurized membrane, the momentum flux force [8] and the viscoelastic dissipation within the membrane [14]. The momentum flux force theory does not specify the physical phenomena responsible for energy loss. It stands that the work of the force corresponding to the nonlinear acceleration of the membrane during the compression phase is not restored during the expansion phase. In a different manner, viscoelastic dissipation corresponds to heat production within the membrane material. This dissipation has been modeled with a linear damping force proportional to indentation velocity [14]. This empirical model did not link explicitly the damping coefficient to the mechanical parameters of the pressurized membrane.

In this paper, we investigate the dependence of the coefficient of restitution with the mechanical properties of the pressurized membrane. We chose to study a thin spherical membrane made of elastomer and inflated with air as a model system. We first present two sets of measurements of coefficient of restitution by systematically varying impact speed and inflation pressure for a small and a large membrane. Second, we observe the part of the pressurized membrane in contact with the ground during the impact and rule out

*loic.tadrist@univ-amu.fr

055001-1

losses by friction. Then, we compare the different predictions of the coefficient of restitution and show that vibrations of the membrane are the main sources of energy losses. This is rationalized combining idealized kinematics of ball impact [15] and a minimal 1-mode vibration modeling. Finally, the dependence of the coefficient of restitution with pressure, impact speed, and membrane mechanical parameters is established.

II. IMPACTS OF PRESSURIZED MEMBRANES: EXPERIMENTS

A. Characteristics of the pressurized membranes

For spherical membranes, we used a set of four small beach volleyballs (BV100 Fun, Decathlon KIPSTA) of deflated radius $R = 8.2 \pm 0.1$ cm, and one large gym ball (gym ball size 3, Decathlon DOMYOS) of deflated radius $R = 31.3 \pm 0.4$ cm [see Fig. 1(a)]. Those spherical membranes were chosen for their minimal composition: they consist of a single layer of elastomer with a valve for inflation. We set the inflation pressure $P - P_{\mathrm{atm}}$ where P is the absolute inner pressure in the membrane and P_{atm} is the atmospheric pressure. The small membrane weighed $m = 179$ g and the large membrane weighed $m = 2.6$ kg. Both membranes had a thickness $e = 2.0 \pm 0.12$ mm. We verified that the mass of the membrane corresponds to $m = 4\pi \rho R^2 e$ with ρ the density of the elastomeric material constituting the membrane.

The membrane elastomer was isotropic and was characterized with a dynamical viscometer to determine the storage modulus E' and loss modulus E''. The pieces of elastomer tested on the viscometer were rectangles of width 9 ± 0.1 mm and length 20.6 ± 0.1 mm. They were clamped on their width and the test temperature was $25\,^{\circ}$C. Over the range of tested frequencies, E' was almost constant $E' \simeq 5.9 \pm 1.0$ MPa and E'' varied linearly with frequency leading to $E''/f = 2\pi \mu \simeq 27 \pm 3$ kPa s, see Fig. 1(b), where μ is the effective viscosity of the material. The Young modulus of the membrane at rest (i.e., $f = 0$ Hz) was $E = 4.2 \pm 0.1$ MPa. The loss modulus was measured on non-prestretched samples of elastomer; see Fig. 1(b). However, when the membrane is inflated, the elastomer is necessarily prestretched. In our conditions, the prestretching of the membrane has been estimated to be smaller than 20% [15] and is expected to slightly decrease the loss modulus E'' [16].

B. Coefficient of restitution as a function of inflation pressure and impact speed

We report here measurements of the impact properties of the pressurized membranes varying impact speed U_0 and inflation pressure $P - P_{\mathrm{atm}}$. Experimental data of the coefficient of restitution for small membranes impacts were already reported in a previous publication [15] but data regarding the large gym ball are original. For both series of measurements, we followed the same protocol where the ball was dropped from a height h on a rigid substrate and a high speed camera allowed us to determine the ingoing and outgoing speeds of the ball, providing an estimate for $\eta = |U_{\mathrm{out}}/U_0|$. A homemade Matlab code detected the circular shape of the membrane. It provided the position of the circle in time
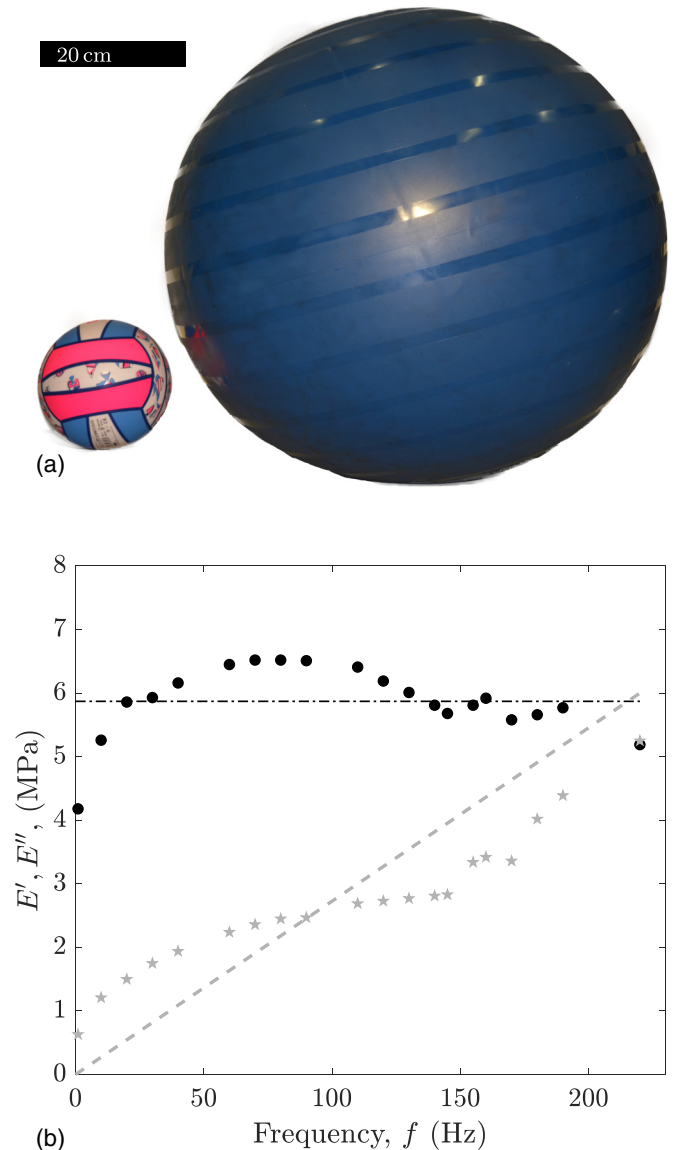

FIG. 1. (a) Small ball and large ball considered as models of pressurized membranes in this paper. (b) Mechanical properties of the elastomer of membranes (BV100 Fun) as a function of forcing frequency with an elongation of 1% and preload of 0.1%. (●): E' and (★): E''. Gray dashed line slope corresponds to $2\pi \mu = 27$ kPa s.

filtering out deformations and vibrations of the membrane. The coefficient of restitution η is plotted in Fig. 2(a) [respectively Fig. 2(b)] as a function of the inflation pressure $P - P_{\mathrm{atm}}$ (respectively impact speed U_0). In the range of low speeds ($U_0 < 2$ m s^{-1}), the coefficient of restitution increases with the impact speed whereas for larger impact speeds $U_0 > 2$ m s^{-1} it decreases. In the following, we focus on impact speeds larger than 2 m s^{-1}. In this range, the coefficient of restitution increases slightly with inflation pressure but decreases with impact speed.

C. Deformations at the contact

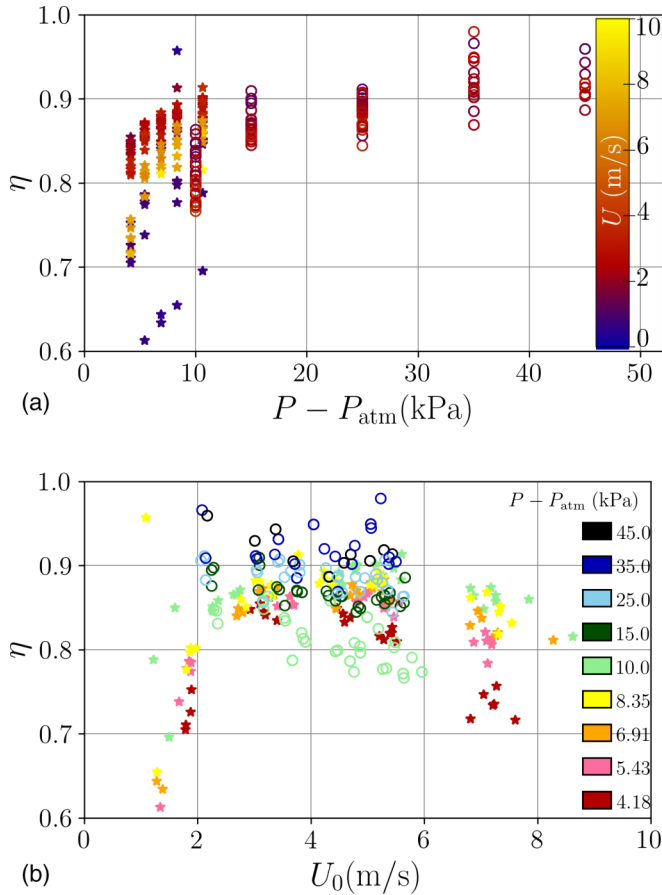Tests of membrane deformation kinematics were carried out on small membranes (BV100 Fun) using a stereo-imaging

FIG. 2. (a) Coefficient of restitution η as a function of inflation pressure $P - P_{\text{atm}}$. Open symbols: Small membrane. Filled symbols: Large membrane. Colors give information about impact velocity. (b) Coefficient of restitution η as a function of impact velocity U_0. Open symbols: Small membrane. Filled symbols: Large membrane. Colors give information about inflation pressure.

FIG. 3. (a) Schematics of the experiment to image membrane displacements at the contact. The pressurized membrane is released from a height h. ① Spherical membrane painted with synthetic Schlieren. ② Imaging facility. ③ Clear window for imaging from below. (b) Parametrization of membrane during contact.

digital image correlation setup (DIC standard 3D, Dantec Dynamics); see Fig. 3(a). The membrane was inflated at recommended pressure $P - P_{\text{atm}} = 15$ kPa. It was then prepared for image correlation: first the ball surface was gently sanded using fine-grained sandpaper to remove superficial paint. The clean white membrane was then finely sprayed black to create a synthetic Schlieren for image correlation.

The setup consisted of a suction device to release the ball without initial velocity or spin from a height h. Suction was produced thanks to a commercial vacuum cleaner. A large glass plate was used as transparent substrate. Lighting and imaging at 300 Hz were done from below. Stereo imaging was performed with two cameras with a slight angle (6°) regarding the vertical.

Image correlation is performed during contact with the glass plate. Figure 4(a) shows that the pressurized membrane is flattened on the ground without crumpling, differently as suggested in the case of basketballs [13]. The deformations show a radial compression of the flattened part of the membrane. The magnitude of the radial compression increases with radial distance.

Figure 4(b) shows the difference between an impact image and the image at the time of largest indentation. The difference
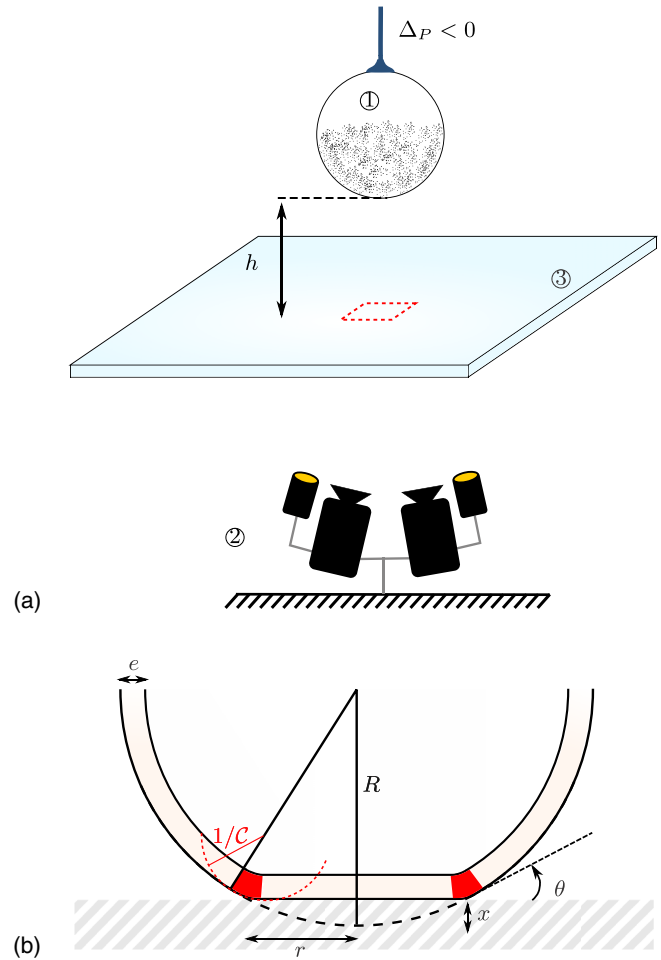
shows a black spot at the contact location indicating that no or negligible slip occurs during the contact of the membrane with the glass plate. If buckling had occurred, this would have created a white spot at the center of the images in Fig. 4(b). One would also notice arrows pointing toward the ring of the fold (with reversal inside the ring) which is not the case; see red arrows in Fig. 4(a). Differently from the contact of rigid spherical shells where buckling occurs [17,18] and involves solid friction, the contact of a pressurized membrane involves neither buckling nor friction in the range of impact conditions explored here.

This difference could result from the fact that internal pressure prevents the buckling transition. The effect of the internal pressure on the onset of wrinkling of an elastic membrane submitted to a point load has been studied by Vella *et al.* [9]. In the limit of high pressure, they showed that wrinkles appear above a critical indentation x_c,

$$\frac{x_c}{R} = 2.52 \frac{(P - P_{\text{atm}})R}{Ee}. \tag{1}$$

Considering typical experimental values used here, $P - P_{\text{atm}} = 15$ kPa, $R = 8$ cm, $e = 2$ mm, $E = 4$ MPa, the
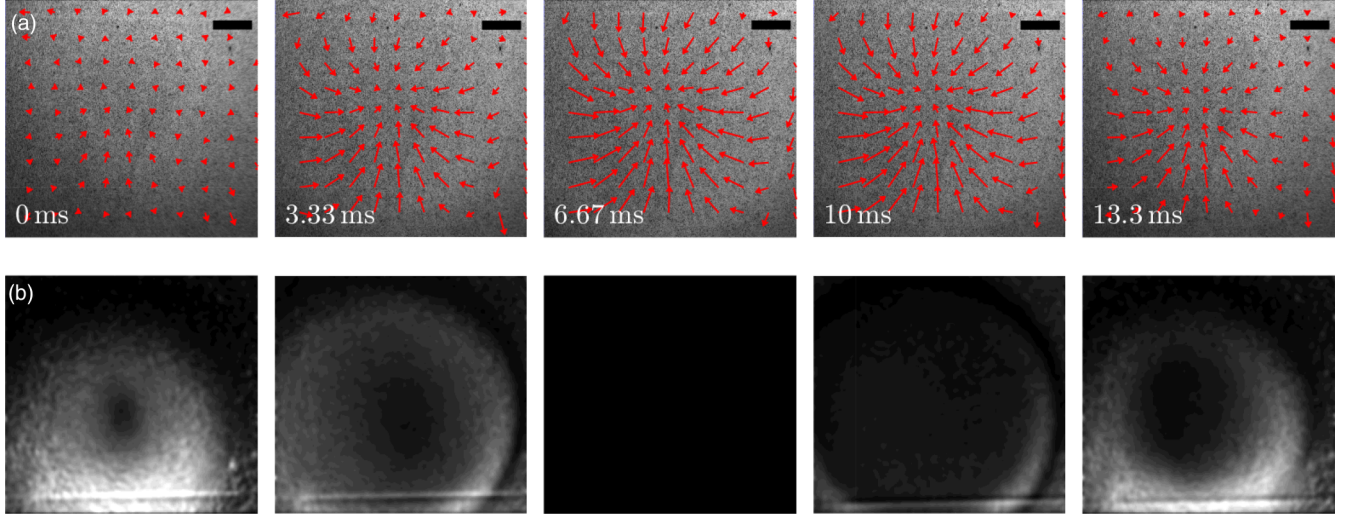
FIG. 4. Contact kinematics of the membrane. (a) Contact area between the ball and the glass plate seen from below at different times after the impact at $t = 0$ ms. Red arrows (not scaled) indicate the compression displacement field computed by digital image correlation. (b) Difference between current image and maximal indentation image at 6.67 ms. Scale bar is 1 cm.

criterion given by Eq. (1) yields $x_c/R \simeq 0.38$. In the range of impact speeds and pressurization explored in this study, the maximal indentation experienced by the pressurized membrane is $x_{\max}/R < 0.20$, and the previous criteria are never reached. This explains why no buckling or wrinkling is observed for sufficiently pressurized membranes in contrast with previous observations made on shells [17]. A scaling similar to that of Eq. (1) arises when considering mirror buckling of the membrane. Pauchard and Rica analyzed mirror buckling by comparing nonbuckled (I) and buckled (II) energies of non-pressurized shells indented on a flat surface. In the nonbuckled state, indentation creates bending in the fold (flat-to-spherical junction) and stretching in the flat section. Differently, when buckled, only bending in the fold is present but with a larger angle. For a nonpressurized shell, energies of states I and II depend on indentation depth x, see Fig. 3(b), and read

$$E_{\mathrm{I}} = \frac{C_0}{4} \frac{E e^{5/2}}{R} x^{3/2} + C_1 \frac{E e}{R} x^3 \quad \text{and} \quad E_{\mathrm{II}} = C_0 \frac{E e^{5/2}}{R} x^{3/2}, \tag{2}$$

where C_0 and C_1 are numerical constants. In order to account for pressurization in this approach, we consider the adiabatic gas compression into the energy balance (no thermal exchange). In state I, gas volume is reduced by the one of the spherical cap approximated by $\pi R x^2$, whereas it is reduced by twice this volume in state II and Eqs. (2) transform as

$$E_{\mathrm{I}} = \frac{C_0}{4} \frac{E e^{5/2}}{R} x^{3/2} + C_1 \frac{E e}{R} x^3 + \pi R (P - P_{\mathrm{atm}}) x^2 \tag{3}$$

and

$$E_{\mathrm{II}} = C_0 \frac{E e^{5/2}}{R} x^{3/2} + 2\pi R (P - P_{\mathrm{atm}}) x^2. \tag{4}$$

Buckling is expected when $E_{\mathrm{I}} > E_{\mathrm{II}}$ which leads to a nonlinear equation with 3 terms,

$$\frac{3 C_0}{4} \frac{E e^{5/2}}{R} x^{3/2} + \pi R (P - P_{\mathrm{atm}}) x^2 - C_1 \frac{E e}{R} x^3 = 0. \tag{5}$$

In the case of pressurized membranes with $C_0 \simeq 0$, the buckling criterion reads

$$\frac{x_c}{R} = \frac{\pi (P - P_{\mathrm{atm}}) R}{C_1 E e}. \tag{6}$$

This approach gives a similar scaling to the one proposed in [9] and suggests that this result does not depend crucially on the geometry of the deformed area. Thus, the conclusion drawn above should be valid for spherical membranes indenting a flat surface, considering a different prefactor.

III. COEFFICIENT OF RESTITUTION OF A PRESSURIZED MEMBRANE

The coefficient of restitution corresponds to a loss of kinetic energy during the impact. This energy may be lost in different manners, either from viscous dissipation in the membrane (in the curved fold or in the stretched flat part), or by transfer to mechanical vibrations of the membrane. The other physical phenomena involved during the impact (sound emission [13], thermal exchange through the membrane [15], and friction/buckling; see above) are much less energetic.

A. Predictions of dissipated power

1. Dissipated power by stretching

During the impact, a fraction of the membrane changes its shape from a spherical shell to a flat surface of radius r [see Fig. 3(b)]. In order to adapt to this change, the membrane must stretch. As the material constituting the membrane is viscoelastic, this deformation induces a loss of energy. In order to estimate this dissipation, we look at the deformation of the membrane during the impact in the region of the fold. Locally, the membrane forms an angle θ with the ground which respects $\sin \theta = r/R$. At this location, a small portion of the spherical part of length ℓ has to compress by a length $\Delta \ell = \ell (\cos \theta - 1)$ to become flat. Thus, the membrane experiences a deformation $\varepsilon_s = \Delta \ell / \ell = \cos \theta - 1$. In the limit
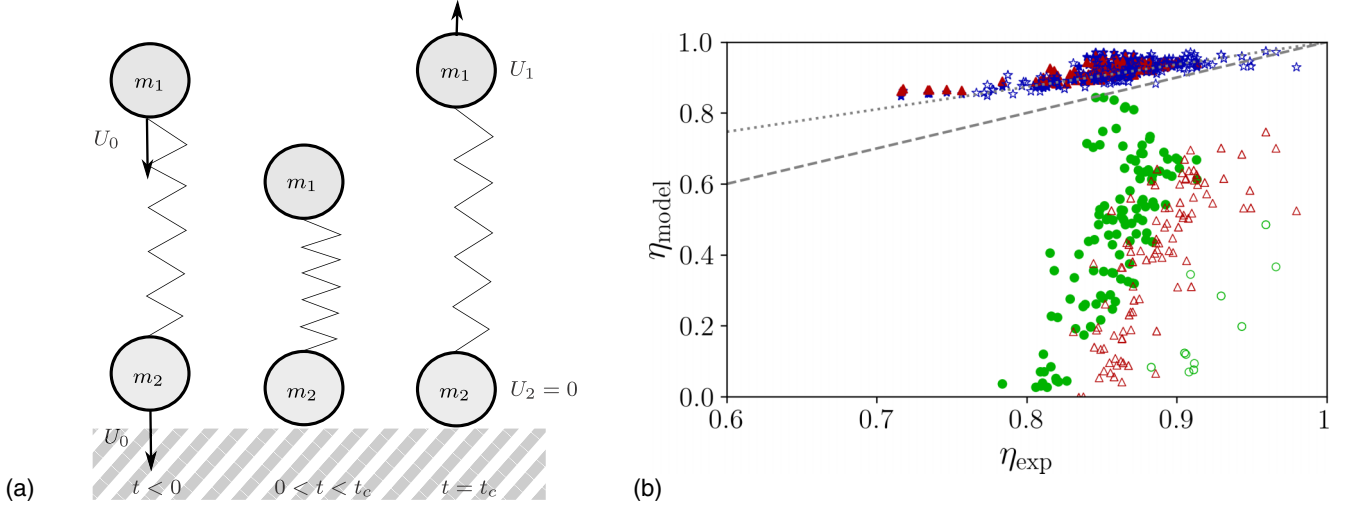
FIG. 5. (a) Toy model of the 2-mass system. (b) Parity plot of Eqs. (16) in green, (17) in red, and (18) in blue. Open symbols correspond to the small membrane and filled symbols correspond to the large membrane. Dashed line: Parity $\eta_{\mathrm{model}} = \eta_{\mathrm{exp}}$. Dotted line: Fit $1 - \eta_{\mathrm{model}} = 0.63(1 - \eta_{\mathrm{exp}})$.

of small indentations ($x \ll R$), corresponding to $\theta \ll 1$, the membrane deformation becomes $\varepsilon_s \simeq -\theta^2/2$ and the angle reduces to $\theta \simeq r/R$. The viscous energy associated to a deformation occurring in a volume dV is $dE_{\mathrm{strech}} = \mu \varepsilon_s \dot{\varepsilon}_s dV$. Considering a portion of the membrane located in the interval r and $r + dr$, the deformation affects a material volume $2\pi r e dr$ and we get the following expression for the power dissipated by stretching,

$$\frac{dE_{\mathrm{strech}}}{dt} = \pi \mu e \frac{r^4 \dot{r}^2}{R^4}. \tag{7}$$

In the limit of small indentations ($x \ll R$), the radius of contact is related to the indentation of the spherical membrane by $r^2 \simeq 2Rx$ [see Fig. 3(b)] and Eq. (7) becomes

$$\frac{dE_{\mathrm{strech}}}{dt} = 2\pi \mu e \frac{x \dot{x}^2}{R}. \tag{8}$$

2. Dissipated power by bending in the fold

The flat part of the membrane is connected to the spherical part of the membrane by a fold. The characteristic size of the fold δ is fixed by a competition between bending and stretching energies as described in [17], leading to $\delta \simeq \sqrt{eR}$. The fold volume is $V_{\mathrm{fold}} = 2\pi r e \delta \simeq 2\pi R \sqrt{2x e^3}$ since the contact radius is $r \simeq \sqrt{2Rx}$ when $x \ll R$. The radius of curvature of the fold scales as $1/\mathcal{C} \sim \delta/\theta$, where $\theta \simeq \sqrt{2x/R}$ is the contact angle of the membrane; see Fig. 3(b). The bending deformations in the fold scale as $\varepsilon_b \sim e\mathcal{C} \sim \sqrt{2xe}/R$ during the typical deformation time $\tau \sim \delta/\dot{r} \sim \sqrt{2xe}/\dot{x}$ that corresponds to the fold dimension divided by the fold velocity. The viscous stresses are thus $\sigma \sim \mu \varepsilon_b/\tau$ where μ is the equivalent viscosity of the membrane. Finally, the dissipated power in the fold scales as

$$\frac{dE_{\mathrm{fold}}}{dt} \sim \mu \frac{\varepsilon_b^2}{\tau^2} V_{\mathrm{fold}} \sim \mu \frac{e^{3/2} \sqrt{x} \dot{x}^2}{R}. \tag{9}$$

3. Dissipated energy by vibrations

Vibrations of the membrane can be described by the vibration modes of a pressurized spherical shell by decomposition of the deformed membrane on spherical harmonics as realized by Feshback *et al.* [19] (p. 1469). To simplify the description of vibrations, we consider a minimal model of two masses connected by a spring; see Fig. 5(a). This model was first developed to describe the rebound of a water droplet impacting a hydrophobic surface [20]. In this model, the first mass, mass 1 located in x_1, corresponds to the mass of membrane that will not contact the ground whereas the other mass, mass 2 located in x_2, corresponds to the amount of membrane that will contact the ground at the maximal indentation of the impact. The two masses m_1 and m_2 are connected by a linear spring of rigidity k and rest length l_0; see Fig. 5(a). Before contact, both masses move with a velocity U_0 toward the ground. When mass 2 makes contact with the ground, it stops ($U_2 = 0$) and mass 1 compresses the spring. The contact ends when the spring recovers its rest length l_0. At this moment mass 2 still has no velocity. We assume that no dissipation occurs in the system, which implies that the total kinetic energy is preserved and mass 1 takes off with velocity $U_1 = \sqrt{1 + m_2/m_1}\, U_0$. The difference in speed between masses 1 and 2 creates vibrations. The vibration energy reads

$$E_{\mathrm{vib}} = \tfrac{1}{2} m_2 U_0^2, \tag{10}$$

where m_2 is the fraction of the membrane of volume $2\pi R e x_{\mathrm{max}}$ in contact with the ground at maximum indentation and which expresses as

$$m_2 = \frac{m x_{\mathrm{max}}}{2R} = \frac{1}{2} \sqrt{\frac{m^3 U_0^2}{\pi R^3 (P - P_{\mathrm{atm}})}}, \tag{11}$$

as the maximal indentation of the membrane expresses $x_{\mathrm{max}} = U_0 \sqrt{m/\pi R (P - P_{\mathrm{atm}})}$ when the dissipation term is neglected [15]. The total energy transferred to vibrations according the

two-mass model is

$$E_{\text{vib}} = \frac{1}{4} \frac{\left(mU_0^2\right)^{3/2}}{\sqrt{\pi R^3 (P - P_{\text{atm}})}}. \tag{12}$$

This energy is ultimately dissipated as heat in the material.

B. Coefficient of restitution in the limit of small dissipation

In this section, we examine the implications of the previous energy dissipation scenarios on the coefficient of restitution. For the sake of simplicity, we assume that the membrane dynamics is not affected by the dissipation. This approximation is motivated by the fact that the pressurized membrane is equivalent to a damped oscillator system with a quality factor larger than 10 ($\eta > 0.7$). In these conditions, the dissipation shifts the natural frequency of the system by less than one percent in relative value. Under these circumstances, the behavior of the pressurized membrane at impact is linear and indentation evolves as [15]

$$x(t) = \sqrt{\frac{mU_0^2}{\pi R(P - P_{\text{atm}})}} \sin\left(\sqrt{\frac{\pi R(P - P_{\text{atm}})}{m}} t\right). \tag{13}$$

In this limit, one can compute the dissipated energy in the membrane from Eqs. (8) and (9),

$$E_{\text{stretch}} = \frac{2\pi \mu e}{R} \int_0^{t_c} \dot{x}^2 x \, dt = \frac{4\mu e m U_0^3}{3R^2(P - P_{\text{atm}})}, \tag{14}$$

$$E_{\text{fold}} = \frac{\mu e^{3/2}}{R} \int_0^{t_c} \dot{x}^2 \sqrt{x} \, dt = 1.61 \frac{\mu U_0^{5/2} e^{3/2} m^{3/4}}{(P - P_{\text{atm}})^{3/4} R^{7/4}}, \tag{15}$$

with $t_c = \pi \times \sqrt{m/[\pi R(P - P_{\text{atm}})]}$. Under these conditions, we derive three predictions for the coefficient of restitution associated with the different origins of dissipation:

$$\eta_{\text{stretch}} = \sqrt{1 - \frac{2E_{\text{stretch}}}{mU_0^2}} \simeq 1 - \frac{4\mu e U_0}{3R^2(P - P_{\text{atm}})}, \tag{16}$$

$$\eta_{\text{fold}} = \sqrt{1 - \frac{2E_{\text{fold}}}{mU_0^2}} \simeq 1 - 1.61 \frac{\mu U_0^{1/2} e^{3/2}}{m^{1/4}(P - P_{\text{atm}})^{3/4} R^{7/4}}, \tag{17}$$

$$\eta_{\text{vib}} = \sqrt{1 - \frac{2E_{\text{vib}}}{mU_0^2}} \simeq 1 - \frac{\sqrt{mU_0^2}}{4\sqrt{\pi R^3 (P - P_{\text{atm}})}}. \tag{18}$$

These three predictions for the coefficient of restitution have different dependencies with the mechanical parameters of the pressurized membrane. Thus, one can hope to distinguish between the three scenarios for energy dissipation by comparing these predictions to experiments. Figure 5(b) presents the parity plot between the predicted coefficient of restitution η_{model} from Eqs. (16), (17), and (18) as a function of the measured coefficient of restitution η_{exp} for small and large membranes, and different inflation pressures and impact speeds. In this representation, experiments match theoretical predictions when data points align on the $y = x$ line (dashed line). We observe that both viscoelastic dissipation models fail in gathering data points showing that this physical background of energy dissipation is unlikely. However predictions of the energy dissipated in the two-mass model gather all data points

on a line $\eta_{\text{model}} - 1 = 0.63(\eta_{\text{exp}} - 1)$ (dotted line). This suggests that the scaling given for energy dissipation is correct although missing the prefactor on mass 2. This conclusion is reinforced by the fact that the agreement is valid over a wide range of parameters: the size of the membrane has been varied by a factor 4, the impacting speed by a factor 8 and the inflation pressure by a factor 9.

IV. DISCUSSION

The fact that the pressurized membrane dissipates the energy into vibrations has several consequences which are discussed in this section. First, the energy dissipated does not depend on the loss modulus μ of the elastomer constituting the membrane [see Eq. (18)]. Thus, the viscoelastic dissipative properties of the membrane do not affect its bouncing quality. Second, Eq. (18) predicts that the coefficient of restitution decreases linearly with U_0 and with $1/\sqrt{P - P_{\text{atm}}}$. This allows us to rationalize the decrease of η with U_0 and its increase with $P - P_{\text{atm}}$ observed experimentally for impact speeds $U_0 > 2$ m s^{-1}.

The expression for the coefficient of restitution given by Eq. (18) relies on several assumptions. First, the pressurized membrane is modeled by two masses connected by a linear spring, a hypothesis that is valid only at small indentations. For large indentations, the nonlinear elastic behavior of the pressurized membrane due to gas compression has to be considered. This effect, described in [15], corresponds to a strain-stiffening behavior; it reduces both contact time and maximal indentation. Compared to the prediction of the linear model, the membrane is expected to be less deformed and thus to dissipate less energy. Second, we assume that the impact dynamics of the pressurized membrane is only marginally modified by the dissipation at small indentations. At larger indentations, energy dissipation would have to be taken into account in the impact dynamics and would modify Eq. (13). Accounting for dissipation in the impact dynamics would increase the contact time.

In the present modeling, we assumed that the inflation-induced prestretching of the membrane was constant and that all results were derived linearly around this reference state. When indentation of the membrane is large, the linear mechanics hypothesis breaks down. The impact becomes nonlinear because of both large displacements with geometrical stiffening [15] and nonlinear material behavior such as strain stiffening or strain softening. The geometrical stiffening would reduce the amount of deformed material and decrease dissipation.

The knowledge of the origin of the dissipation in the impact is interesting for practical situations where low or high coefficients of restitution may be required. For impact protection applications, a low coefficient of restitution helps to reduce the amount of momentum exchanged during the impact. When a pressurized membrane of mass m impacts onto a massive ground, the change of momentum of the membrane is $2mU_0$ in a perfectly elastic case, twice the exchange of momentum that occurs during a perfectly inelastic impact mU_0. For sport balls, a minimal coefficient or restitution is prescribed by the rules in order to ensure that the ball can be released with sufficient speed. In sports, a maximal inner pressure is also

prescribed (which corresponds to a maximal coefficient of restitution for a given impact speed). This may be related to the decrease of contact time as the inner pressure increases. This change of contact time increases the rate of exchange of momentum (i.e., impact inertial forces) and thus the severity of impact-related damages. It also reduces the possibility for the player to control the ball trajectory during contact.

This study considers the origin of dissipation when a pressurized membrane impacts a rigid ground. The coefficient of restitution of small and large inflated membranes has been measured for a wide range of internal pressures and impact speeds. Four possible sources of energy dissipation in this problem have been considered. Solid friction has been discarded by performing image visualization in the contact area. The other possible sources of dissipation are the compression of the flattened membrane, the bending of the viscoelastic membrane in the fold, and the energy transferred to vibrations. A physical prediction for each dissipation scenario has been computed and compared to measurements. The deformation of the pressurized membrane during the impact was considered through the framework of linear mechanics around the reference state of the pressurized shell. Impact-induced deformations are mainly the consequence of the impact kinematics.

Based on experimental data, we concluded that during the impact of a pressurized membrane with a rigid ground, the energy is dissipated in vibrations and this may be predicted by a two-mass model. Identifying the source of dissipation in this problem should help in improving the design of impact protections and a better understanding of the role of ball inflation pressure in sport. This work opens multiple perspectives as improving the modeling of membrane vibrations beyond the simple model of two masses connected by a linear spring, characterizing the membrane vibrations after impact which is challenging from a technical point of view and considering the effect of the impactor geometry on the dissipation that takes place during impact.

[1] H. Zhou, Z. Zhong, and M. Hu, Design and occupant-protection performance analysis of a new tubular driver airbag, Engineering **4**, 291 (2018).

[2] M. Kurt, K. Laksari, C. Kuo, G. A. Grant, and D. B. Camarillo, Modeling and optimization of airbag helmets for preventing head injuries in bicycling, Ann. Biomed. Eng. **45**, 1148 (2017).

[3] N. Mills, Running shoe materials, Materials in Sports Equipment **1**, 65 (2003).

[4] K. Baousi, N. Fear, C. Mourouzis, B. Stokes, H. Wood, P. Worgan, and A. Roudaut, Inflashoe: A shape changing shoe to control underfoot pressure, in *Proceedings of the 2017 CHI Conference Extended Abstracts on Human Factors in Computing Systems* (ACM, 2017), pp. 2381–2387.

[5] B. Nemeth, M. van der Kaaij, R. Nelissen, J.-K. van Wijnen, K. Drost, and G. J. Blauw, Prevention of hip fractures in older adults residing in long-term care facilities with a hip airbag: A retrospective pilot study, BMC Geriatrics **22**, 1 (2022).

[6] J. Krauel and N. Ferguson, *Inflatable: Art, Architecture, and Design* (UNKNO, 2013).

[7] R. B. Malla and T. G. Gionet, Dynamic response of a pressurized frame-membrane lunar structure with regolith cover subjected to impact load, J. Aerospace Eng. **26**, 855 (2013).

[8] W. Stronge and A. Ashcroft, Oblique impact of inflated balls at large deflections, Int. J. Impact Eng. **34**, 1003 (2007).

[9] D. Vella, A. Ajdari, A. Vaziri, and A. Boudaoud, Wrinkling of Pressurized Elastic Shells, Phys. Rev. Lett. **107**, 174301 (2011).

[10] M. Taffetani and D. Vella, Regimes of wrinkling in pressurized elastic shells, Philos. Trans. R. Soc. A **375**, 20160330 (2017).

[11] W. J. Stronge, *Impact Mechanics* (Cambridge University Press, 2018).

[12] R. Cross, Dynamic properties of tennis balls, Sports Eng. **2**, 23 (1999).

[13] J. Katz, Thump, ring: The sound of a bouncing ball, Eur. J. Phys. **31**, 849 (2010).

[14] A. Georgallas and G. Landry, The coefficient of restitution of pressurized balls: A mechanistic model, Can. J. Phys. **94**, 42 (2015).

[15] L. Tadrist, B. D. Texier, F. Lanzetta, and L. Tadrist, Impact of a pressurised membrane: Contact time, Int. J. Impact Eng. **156**, 103963 (2021).

[16] Q. Guo, F. Zaïri, H. Baraket, M. Chaabane, and X. Guo, Pre-stretch dependency of the cyclic dissipation in carbon-filled SBR, Eur. Polymer J. **96**, 145 (2017).

[17] L. Pauchard and S. Rica, Contact and compression of elastic spherical shells: The physics of a ping-pong ball, Philos. Mag. B **78**, 225 (1998).

[18] R. Cross, Impact behavior of hollow balls, Am. J. Phys. **82**, 189 (2014).

[19] H. Feshbach, P. M. Morse, and M. Michio, *Methods of Theoretical Physics* (Dover Publications, 2019).

[20] A.-L. Biance, F. Chevy, C. Clanet, G. Lagubeau, and D. Quéré, On the elasticity of an inertial liquid shock, J. Fluid Mech. **554**, 47 (2006).